



# Vibration Analysis of Double Deck Floating Roof of Storage Tank in Cases of Tube, Ordinary and Thickened Foam Seals

H. Ahmadi<sup>\*a</sup>, M. H. Kadivar<sup>b</sup>

<sup>a</sup> International College, Shiraz University, Shiraz, Iran

<sup>b</sup> School of Mechanical Engineering, Shiraz University, Shiraz, Iran

## PAPER INFO

### Paper history:

Received 23 January 2022

Received in revised form 11 April 2022

Accepted 01 May 2022

### Keywords:

Slosh

Finite Element

Vibration Mitigation

Fluid-structure Interaction

Earthquake

## ABSTRACT

Vibration of a floating roof in cases of tube and foam seals has been analyzed by ANSYS. Fluid-Structure Interaction (FSI) and sloshing phenomenon have been considered. Modal responses, time waves and frequency spectrums of the roof vibrations in the two sealing cases were evaluated during horizontal seismic excitation of the tank base. Then, the effects of the main mechanical factors of the seal on the roof vibration were investigated. The roof vibration amplitude in the foam sealing case was considerably lower than that in the tube sealing case due to more damping of the foam seal. Also, the foam sealing case had higher natural frequency than the tube sealing case due to more tank-axial (vertical) shear modulus of the foam seal in relative to the tube seal. Regarding this result, the foam seal was vertically added by 50% and the tank base was seismically excited again. It was seen that this improvement in thickness has more contribution to the floating roof vibration mitigation.

doi: 10.5829/ije.2022.35.07a.18

## NOMENCLATURE

$b$	Initial gap between the roof and shell	$\sigma_t$	Tube shell stress
$[C]$	Proportional damping matrix	$\delta$	Kronecker delta
$E$	Instantaneous modulus of elasticity	$\zeta$	Damping ratio
$F$	Force	$\rho$	Density of the tank liquid (kg/m <sup>3</sup> )
$[F]$	Seismic forces matrix	$\lambda$	Sloshing height
$g$	Gravity (m/s <sup>2</sup> )	$\tau$	Tube shell thickness
$h$	Height the liquid inside the tube seal	$\mu$	Friction coefficient
$[M]$	Mass matrix	$\eta$	Loss factor
$K$	Stiffness	$\epsilon$	Strain
$[K]$	Stiffness matrix	$\omega$	Rotational frequency
$p$	Pressure	<b>Subscripts</b>	
$[P]$	Pressure matrix	$f$	Tank liquid
$[R]$	Fluid-structure coupling matrix	$j$	Annular sector number
$\Delta u$	Gap size change	$i$	Principle axis
$[U]$	Structure displacement matrix	$l$	Liquid inside the tube
$\Delta W$	Energy loss	$n$	Normal direction
$W_0$	Input energy	$s$	Solid
$\Delta x$	Roof horizontal displacement	$sy$	Tangential tank-axial direction
<b>Greek Symbols</b>		$sz$	Tangential circumferential direction
$\sigma$	Stress tensor	$t$	Tube shell

## 1. INTRODUCTION

In oil industries, hydrocarbon storage tanks must have floating roof in order to prevent vaporization and loss of

the products that may also be flammable or hazardous to the environment. There are two types of floating roof: Single Deck Floating Roof (SDFR) and Double Deck Floating Roof (DDFR). A SDFR is made up of a single-

\*Corresponding Author Email: ahmadihs1354@gmail.com (H. Ahmadi)

layer deck plate at the roof center and an annular bulk named pontoon around the deck plate. A DDFR consists essentially of a lower deck, an upper deck and some stiffeners between them. In Figure 1, the lower deck and stiffeners are demonstrated. In addition, a segment of a DDFR and an overall view of some roofed tanks can be seen in Figures 2 and 3. Refer to the descriptions represented by Ahmadi and Kadivar [1] and also by Kuan [2] about the storage tanks and floating roofs.

On the other hand, there is a gap between the floating roof and the tank shell in order to facilitate tank-axial (vertical) movement of the roof when the liquid rises up and falls down. However, this gap should be filled with a seal to prevent the liquid escape through this area. Arrangement of a roof seal relative to the tank shell and floating roof has been demonstrated in Figure 2.

Earthquakes produce long-period oscillations on the liquid surface of storage tanks, which is called sloshing phenomenon [3]. Slosh induces vibration to the floating roof through Fluid-Structure Interaction (FSI). Such seismic oscillation may result in consequences such as sinking of the roof, destructive fire of the products or splash of the toxic liquid to the environment. Some events due to the roof slosh have been mentioned in the studies provided by Chang and Lin [4], in other studies by Hatayama [5] and Ahmadi and Kadivar [1]. Figure 3 shows some floating roofed tanks in Tomakomai during 2003 Tokachi-oki earthquake. In this Figure, open-top fire happened in tank 'b', i.e. the fire spread to all parts of the roof. Usually in such events, the tanks catch fire due to the sparks generated by up down movement of the roof against the seal and shell.

Hence, seismic vibration of the floating roof of the storage tank has been taken into consideration as an important problem in many studies. In this way, several attempts were made toward vibration mitigation of the floating roof vibration and risk assessment of petroleum storage tanks [6-9]. However, so far, the floating roof outer rim was modeled as a free or fixed boundary condition or with radial only-compression springs. Salarieh et al. [10] modeled deck plate as a flexural element rather than membrane. Shabani investigated the induced stresses in SDFR of some seismically-excited storage tanks [11]. Yoshida et al. [12, 13] considered a free peripheral boundary for a floating roof to investigate sloshing characteristics of a storage tank. Golzar et al. [14] analyzed the slosh of a storage tank floating roof under different earthquakes. In these investigations, the moments and shear modulus of the floating roof edges have been taken equal to zero. Shabani and Golzar [15] assumed zero axial traction for computation of the seismic deflection of a floating roof. Goudarzi [16] studied the second seismic vibration mode of a floating roof by considering free-edge boundary for the roof. Goudarzi [17] studied the attenuation effect of a SDFR by assuming free-edge boundary for the roof. He [18]

also proposed a practical seismic procedure for evaluating the sloshing response and the dynamic stresses inside a DDFR subjected to seismic excitation. The roof edge was also assumed free in this study. Meera and Reshmi [19] studied the SDFR vibration regarding different patterns for the SDFR stiffeners. They assumed



**Figure 1.** Lower deck and floating roof stiffeners configuration (courtesy of Kavan Sadid Sanaat Koosha)

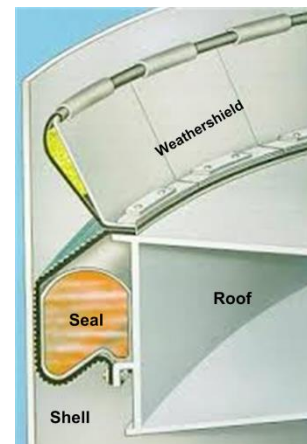


**Figure 2.** Arrangement of a roof seal relative to the tank shell and the floating roof



**Figure 3.** Open top fire in a crude oil tank [5]

fixed boundary for the roof. The stress pattern of a circular SDFR and a DDFR with free edges under a seismic excitation was illustrated by Golzar et al. [20]. Belostotsky et al. [21] considered all the essential parts of the storage tank in their analysis. The roof seal was modeled as radial only-compression springs. However, the numerical results of such research have not been represented. Hosseini et al. [22] studied the seismic vibration of the storage tank assuming a rigid disk as the floating roof and some radial only-compression springs as the seal.

The aforementioned studies were only devoted to the analysis of the roof vibration. In some other researches, several vibration suppression approaches were also applied to the roof and were evaluated by conventional analytical or numerical procedures. Sakai and Inoue [23] proposed some isolating rubbers between the layers of the pontoons of a SDFR in order to reduce seismic vibration. Utsumi [6] studied the effect of a vibration absorber including mass, damper and spring on a SDFR vibration. Kobayashi and Sato [7] designed a vibration absorber which have a U-shaped tube in addition to mass, damper and spring for passive vibration control of the roof. Hasheminejad and Mohammadi [8] discussed an active control method for vibration mitigation of a floating roof. Hosseini et al. [24] conducted an experimental study using a Suspended Annular Baffle hanging from the floating-roof to reduce the maximum sloshing height. Ruiz et al. [25] proposed a new type of liquid mass damper, called tuned liquid damper for vibration attenuation of the roof. However, the above analysis was conducted with no seal existence. In this work, the seal parameters will be taken into account for vibration suppression of the floating roof.

As described above, in most of the studies in the literature, vibration of the floating roofs have been investigated regarding free or fixed edge for the roof. In other words, the seal was neglected in the analysis. It is obvious that the boundary condition is an essential parameter for solution of a structural dynamic system. Therefore, considering free-edge boundary condition, as was assumed in most of the aforementioned works, makes a substantial deviation from the actual sloshing condition of the floating roof.

In some other scarce studies, the seal was modeled as radial only-compression springs ignoring the seal stiffness in the other directions. The main contribution of the seal radial forces is to improve the sticking condition by increasing the friction forces at the seal-shell contact. However, friction forces of the seal must be limited such that it does not prevent the roof slipping during the liquid level change. In the present work, the effect of slipping to the roof sloshing will be discussed in addition to the radial elastic modulus effect.

Sloshing occurs in the vertical direction. Therefore, the vertical forces will have some contribution to the

sloshing. In addition, the tangential vertical forces can rapture the sticking condition of the seal changing the roof deformation pattern. Therefore, the stiffness of the seal in the vertical direction can be revised in order to suppress the floating roof sloshing. On the other hand, the radial space between the roof edge and the wall is small relative to the roof radius. Therefore, the seal shear stress can also be effective in the sloshing of the roof. Ahmadi and Kadivar [1] investigated seismic vibration of a floating roof by considering the main mechanical properties of the seal including shear and elastic modulus in all directions. However, the contribution of the seal stiffness in each Degrees of Freedom (DoF) was not clarified. Therefore, in the present work, the contribution of the modulus of the seal to the DDFR vibration will be discussed in the all DoFs including vertical shear modulus .

Damping is another essential factor in the vibration suppression of the dynamic systems. As the seal incorporates in the roof vibration through the roof peripheral boundary, the seal damping can affect the roof vibration. Hence, an attempt will be made to use the seal damping to reduce the roof vibration .

Mass is another factor that contribute to the vibration of a flexible system through the effective and modal masses. The attachment of the seal to the roof periphery incorporates the seal mass in the roof mass configuration. As the seal volume is constant in the default design, the effect of the seal density on the roof slosh will also be investigated in the present study.

Several types of seals are used in the oil industries. Tube and foam seals are the two conventional ones, which are used in this study. Fundamental characteristics of the other seals can be extracted through analysis of these two seals. A tube seal, as its name suggests, is a tube containing liquid which is used for sealing the roof peripheral gap. A foam seal is a cover with suitable foam inside it that is used for the same purpose. Figure 4 shows overall configuration of these two types of seal.

Regarding the above descriptions, the following parameters of the foam and tube seal are more impressive.

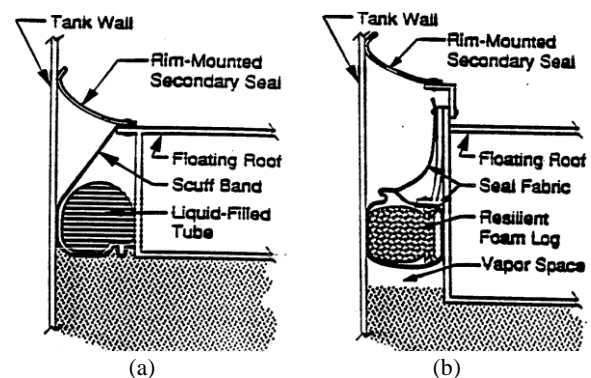


Figure 4. (a) A typical tube seal, (b) A typical foam seal

1. Foam has more shear modulus than water. Therefore, generally, a foam seal has more shear modulus than a tube seal in a similar sealing mechanism.
2. Radial modulus of the foam seal will be extracted from the properties of the conventional foams. Radial modulus of the tube seal will be computed numerically. However, regardless of the seal type, the seal radial forces must be limited in a range in order to facilitate vertical movement of the roof during water level change.
3. Damping of the foam seal is more than tube seal due to the hysteresis damping present in the foam during vibration.
4. The tube seal mass is more than the foam seal mass as water has more density than foam.
5. The slipping condition depends on the radial forces and is independent of the seal type as described so far. Hence, the slipping effect on the roof sloshing will be investigated regardless of the seal type.

As described so far, free boundary condition was assumed in about 90% of the previous works for floating roof vibration analysis, and in some other studies radial springs has been considered, while slosh movement is in the vertical direction and peripheral friction can resist such movement. Hence, the novelty of the present work is to analyze and optimize the contribution of a boundary condition including the damping and vertical shear modulus of the seal and slipping or sticking condition at this area. For this purpose, vibration of a DDFR will be evaluated in the two cases of tube and foam seal considering the main mechanical parameters of the seal which was described so far. Furthermore, according to the achieved results, a new method for DDFR vibration mitigation will be recommended and discussed.

## 2. THEORIES OF THE ROOF VIBRATION WITH CONTACT SEALS

In ANSYS Parametric Design Language (APDL), numerical simulation of the fluid in terms of the dynamic pressures and Fluid-Structure Interaction (FSI) in a fully coupled manner as well as sloshing phenomenon is possible [26]. Fully coupled method facilitates the solution of the problem by one equation. However, it spends more solution time than loosely coupled approach, although the result of the former approach is more exact. The fundamental of FSI is the structure deformation and the fluid forces. Refer to the descriptions provided by Sigrist [27] for more detail about the type of fluid-structure coupling methods. In a storage tank with a floating roof, sloshing phenomenon exists at the roof-liquid interface in addition to FSI according to the following relation.

$$p_{slosh} = -\rho_f g \lambda \tag{1}$$

Therefore, in the sloshing surface, the displacement-based stiffness matrix due to gravity can be added to the coupled system of elemental equations as:

$$\begin{bmatrix} [M_s] & 0 \\ \rho_f [R^T] & [M_f] \end{bmatrix} \begin{Bmatrix} [\ddot{U}] \\ [\ddot{P}] \end{Bmatrix} + \begin{bmatrix} [C_s] & 0 \\ 0 & [C_f] \end{bmatrix} \begin{Bmatrix} [\dot{U}] \\ [\dot{P}] \end{Bmatrix} + \begin{bmatrix} [K_s] + [K_{slosh}] & -R \\ 0 & [K_f] \end{bmatrix} \begin{Bmatrix} [U] \\ [P] \end{Bmatrix} = \begin{Bmatrix} [F] \\ 0 \end{Bmatrix} \tag{2}$$

However, boundary condition around the roof must also be considered in this regard. As stated before, floating roof edges are connected to the seals.

One of the distinct mechanical characteristic of the tube seal is its normal pressure behavior versus displacement that can be considered as the seal elasticity according to the following relation.

$$\sigma_{ii} = -p_t \delta_{ii} \tag{3}$$

It will be shown that this property is not so effective in the roof vibration. Therefore, a simple model has been used for it as follows. The tube seal around the roof is divided into some annular sectors. Location and nomenclature of a typical sector has been demonstrated in Figure 5. Then, the average total pressure of the tube in each discretized time step is estimated as the sum of the average static pressures due to the liquid weight in the tube and the hoop stress of the tube shell. The idea behind the hoop stress calculation is the relation represented by Beer et al. [28] for thin-walled circular pressure vessels. However, in this subject, tube seal cross section will expand in the form of a right triangle due to the limitations provided by scuff band as demonstrated in Figure 6. Therefore, a direction correction is applied to the relation derived by these authors as follows.

$$p_j = \rho_l g \left( \frac{h}{2} + \Delta h \right) + \frac{\sigma_t \tau}{(b - \Delta x)} \left( 1 + \frac{\Delta h}{\sqrt{(b - \Delta x)^2 + (\Delta h)^2}} \right) \tag{4}$$

As can be seen in Figure 6, the maximum variation of the tube seal height ‘ $\Delta h$ ’ due to ‘ $\Delta x$ ’ roof progression is on the right of the triangle. Assuming constant volume of water in the tube sector during the roof progression, this value can be calculated by the following equation.

$$h \Delta x = \frac{(b - \Delta x) \Delta h}{2} \tag{5}$$

which leads to

$$\Delta h = \frac{2h \Delta x}{b - \Delta x} \tag{6}$$

The left hand side of Equation (5) is the water regression in the tube, and the right hand side is water rise through the scuff band triangular hollow space. Note that the bottom side of the scuff band is under the liquid or vapor

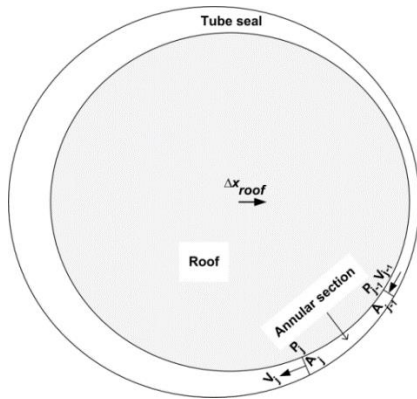


**Figure 5.** Location and fluid nomenclature of an annular sector of a tube seal

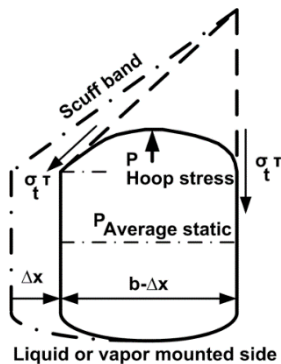


**Figure 6.** Tube seal behavior during deformation

However, Equation (4) does not comply with the laboratory condition of the stress-strain test, as the water escape from the sectors in the circumferential direction ‘sz’ is considered zero. This flow blocking assumption must be compensated in the form of Poisson’s ratio. In this regard, the Poisson’s ratio is involved in the non-linear stress-strain relation according to Hook’s law for multiaxial loading of the homogeneous materials [28].

$$\epsilon = \frac{\sigma_n}{E} - \nu \frac{\sigma_{sz}}{E} \tag{7}$$

Assuming uniform hydrostatic pressure in the tube sector ‘j’ and using equations (3) and (7), the strain can be represented in terms of the hydrostatic pressure as

$$\epsilon_j = \frac{p_j(1-\nu)}{E_j} \tag{8}$$

Having Poisson’s ratio, strain and pressure, the instantaneous elastic modulus can be derived from the above equation.

In Equations (4-8), non-linear relations between the stress and strain of the tube seal were established. Foam seals also have non-linear stress-strain relationship, i.e. elasticity of the foam seal depends on the regions in which the stress applied to it. In this regard, the elasticity

behavior of the foams can be classified into three regions: linear elastic, plateau and densification as indicated in Figure 7 [29]. Generally, polyurethane foams are used for floating roof sealing.

The seal foam is installed in the roof-shell gap with an initial pre-compression. This pre-compression moves the stress-strain operating condition to the plateau region. Therefore, the foam seals generally work in the plateau region.

Another distinct property of the foam is vibration absorption. Foam behaves differently in loading and unloading. As Figure 8 shows, the area between the loading and unloading curve is the energy loss due to the hysteresis loop. This property makes the foam to be a type of viscoelastic material. Viscoelasticity of the foam can reduce the roof vibration through hysteresis energy loss. Hence, damping effect of the foam seal to the roof vibration has been discussed. The loss factor due to the foam hysteresis can be computed from the following equation.

$$\eta = \frac{\Delta W}{2\pi W_0} \tag{9}$$

According to the loss factor, damping ratio can be calculated as

$$\zeta = \frac{\eta}{2} \tag{10}$$

However, the seal participates in the roof vibration only if it is in the closed contact with the tank shell. Closed and open contact depends on the following relations.

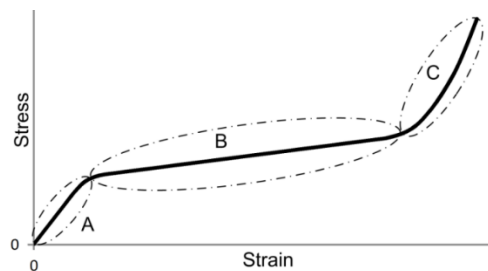


**Figure 7.** Stress-strain curve of a polyurethane foam in (a) linear elastic, (b) plateau, (c) densification regions

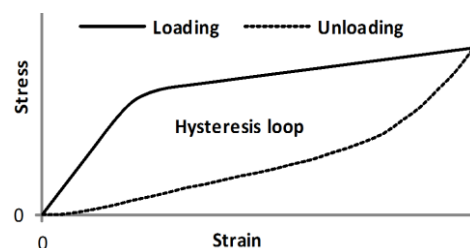


**Figure 8.** Representation of the hysteresis damping in the foam seals

$$F_n = \begin{cases} 0 & \text{if } \Delta u_n > 0 \text{ (Open Contact)} \\ K_n \Delta u_n & \text{if } \Delta u_n \leq 0 \text{ (Closed Contact)} \end{cases} \quad (11)$$

There are two cases of the closed contact: sticking or slipping. In sticking, the tangential movement is only due to the flexibility of the contact materials. On the other hand, slipping occurs if the vertical forces on the contact area exceed tangential friction forces [26]. This principle can be represented by:

$$F_{sy} = \begin{cases} K_{sy} \Delta u_y & \text{if } \sqrt{F_{sy}^2 + F_{sz}^2} - \mu F_n < 0 \\ & \text{(Sticking)} \\ \mu K_n \Delta u_n & \text{if } \sqrt{F_{sy}^2 + F_{sz}^2} - \mu F_n = 0 \\ & \text{(Slipping)} \end{cases} \quad (12)$$

### 3. TANK AND FLOATING ROOF SPECIFICATIONS

A cylindrical storage tank with a DDFR is considered for analysis. Tank body and DDFR specifications are selected according to Siraf storage tank located in south of Iran. The content of the storage tank is natural gas condensate. The general specifications of the storage tank and shell are summarized in Table 1.

Floating roof dimensions are also given in Table 2. Lower and upper decks of the roof are stiffened by bulkheads, trusses and rafters. Bulkheads are dividing walls for separation of the radial and annular compartments.

So far, all the essential parts of the roof, liquid and tank shell have been introduced. The objective is to study and compare the vibration of the roof in the two sealing cases of the tube and foam seal. Therefore, dimensions and mechanical characteristics of these two types of seal are required, which will be introduced in the next section.

**TABLE 1.** Storage tank general and shell specifications

Parameter	Value
Tank height	14 m
Tank diameter	60 m
Liquid density	648 kg/m <sup>3</sup>
Liquid Viscosity	8.9e-4 Pa.s
Rated wall thickness	0.02 m
Liquid height considering sufficient freeboard	12 m
Metal density	7850 kg/m <sup>3</sup>
Metal Young's modulus	2e11 N/m <sup>2</sup>
Metal Poisson's ratio	0.3

**TABLE 2.** Floating roof dimension

Parameter	Value
Height	0.672 m
Upper deck thickness	0.00477 m
Lower deck thickness	0.00637 m
Height in contact with seal	0.40 m
Gap between roof rim and shell	0.20 m

### 4. MECHANICAL SPECIFICATIONS OF THE TUBE AND FOAM SEAL

The internal envelope of the tube seal is the shell that holds the water. The outer envelope is the scuff band, which supports the tube against rubbing and collapsing. The thickness of the tube shell has been taken 2mm while the scuff band has been considered as a fixture that will be described later.

The behavior of the tube seal during a horizontal simulating motion of the roof has been modeled as follows:

1. The tube is filled with water after installation. The hydrostatic pressure produced in this step is considered as the initial stress of the seal. This value was 1970 Pa.
2. The total length of the tube, which is equal to the roof circumference, has been divided into 16 annular sectors.
3. The horizontal movement of the roof relative to the tank shell during an earthquake has been modeled as small displacements applied to the roof in very short time segments.
4. These small movements change the liquid level of the tube. This increases the hydrostatic pressure. In addition, a static pressure will be generated due to the tensions produced in the tube shell. The total stress of the seal is equal to the sum of these two values that is computed by Equation (4).
5. Lateral scape of the water from the sectors has also been considered as Poisson's ratio involvement according to Equation (8).

Different time segments have different displacements, as mentioned in Table 3 for the first quadrant. Such sequence of pressure variation is repeated in the other quadrants. In each sector, horizontal motion of the roof is different as can be distinguished from Figure 5. Thus, each sector will have distinct stress-strain relationship. Table 3 expresses the pressures of each sector resulted from the horizontal displacements applied to the roof.

Poisson's ratio has been taken equal to 0.5 which is Poisson's ratio of water as the main part of the tube. Using Table 3, non-linear relations between the stress and strain of the tube seal were established for each sector. The strains were calculated by non-dimensional

**TABLE 3.** Tube seal pressure in the first quadrant in pascal

Horizontal displacement of the roof	0.006	0.0048	0.0036	0.0024	0.0012	
1	27087	20861	15285	10307	5881	
Sectors in the first quadrant	2	22382	17448	12970	8916	5255
3	14615	11700	8988	6468	4129	
4	6108	5197	4329	3501	2712	

quantities of the displacements in Table 3. Using the strains and the pressures summarized in this table, instantaneous stresses were derived from Equation (8). The above values were introduced to the macro in table format. Damping ratio of the tube seal was considered 0.05 that is approximately equal to the natural rubber damping affected by the fluid friction inside the tube.

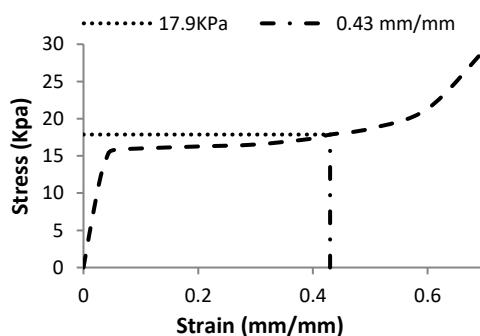
For tube and foam seal comparison, the stress-strain curve of the selected foam seal is shown in Figure 9. The governing stress-strain relationship has been estimated considering reasonable stiffness of the foams provided by some manufacturers [30].

Damping of the seal was estimated according to the usual hysteresis loops present in polyurethane (PU) foams [29] and using Equations (9-10). Based on these considerations, damping ratio of the foam was estimated 0.15.

The foam seal is also installed by an initial compression. An initial compressive stress of 17.9KPa has been considered for the foam seal. Having the stress value, the initial compressive strains can be obtained from Figure 9 as:

$$\varepsilon_0 = 0.43 \text{ mm / mm} \quad (10)$$

In addition, some retainers are used to install the seal, as demonstrated in Figure 4. Tube and foam seals both have weather shield and envelope. Weather shield protects the seal against harsh environment. Tube shell in the tube seal and foam envelope in the foam seal affect

**Figure 9.** Stress-strain diagram of the foam seal with initial stress and strain

the mechanical characteristics of the seal in the same way. In addition, scuff band holds the tube seal to protect it from wear and tear. For foam seal, similar apparatus is used instead of the scuff band. According to the aforementioned descriptions, the fixtures used for holding the tube and foam seals have approximately the same mechanical properties. Hence, equal elastic and shear modulus have been added to the tube and foam seals due to the presence of the fixtures.

## 5. MODELING AND MESHING

A macro using APDL has been provided to perform finite element analysis of the fluid and structures of the tank. 99618 elements have been used in the model. The basic of this work is similar to the study that was performed by Ahmadi and Kadivar [1]. In addition, slosh and seal-shell contact models have been improved. Also, some details about the floating roof and slosh modeling have been introduced. In Figures 10 and 11, exploded views of the finite element model of the tank system are illustrated. Figure 10 includes the main roof parts and a layer of the liquid elements. In Figure 11, shell, liquid, seal and contact elements have been demonstrated.

For liquid meshing, three dimensional (3-D), 8-node wave elements have been used. In the elements inside the fluid, the pressure-based wave equation are established. FSI was applied at the shell-liquid and the roof-liquid interfaces. At such areas, displacement DoFs are also activated. All nodes of the upper surface of the liquid are located so that they coincide with the corresponding roof nodes in the radial and angular directions. This condition facilitates FSI for the roof-liquid common boundary. In Figure 11c, a sector of the lower deck has been added to the upper surface of the liquid to show the node coincidence. Then, meshing coincidence was extended to the lower liquid levels to produce liquid elements, and to the stiffeners and upper deck as illustrated in Figure 12. In addition to FSI, slosh condition must also be provided at the nodes of the upper surface of the liquid. Note that only dynamic pressure is involved in the liquid modeling.

The seals are fixed to the floating roof perimeter while it can move relative to the tank shell that is in contact with it. 4-node 3-D interface elements have been used to model the seal. This type of element is generally suitable for modeling the washers and gaskets such as the current application. Both the tube and foam seals are approximately equal in dimension. For this reason, the same element shape has been selected for both of them.

Contact element is another factor that involves in the roof vibration. There are several methods for modeling the contact elements, from which 3-D node-to-node contact elements have been used. Penalty method has been taken into account for solution of the contact parameters. The method of calculating the normal, i.e.

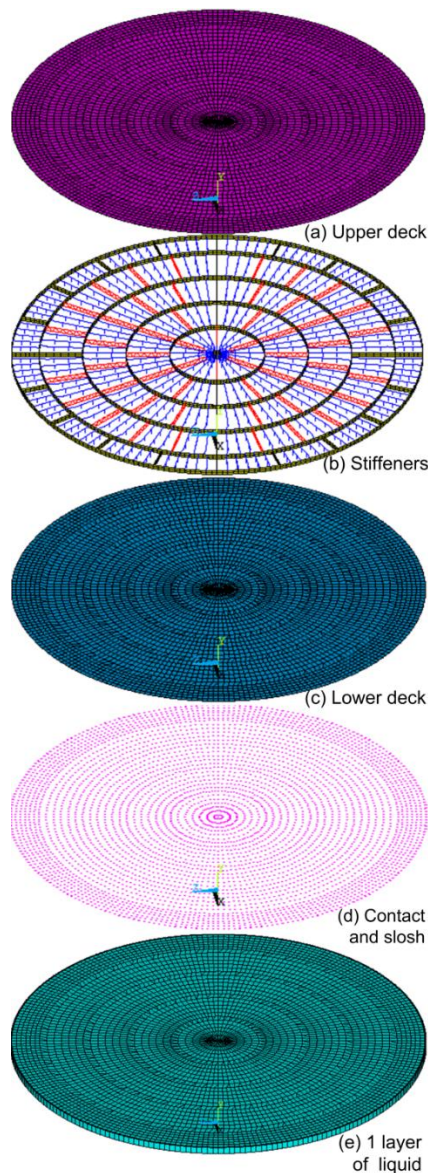


**Figure 10.** Exploded finite element model of the roof and its adjacent liquid

tank radial direction, and tangential forces was depicted in Equations (11-12). Contact forces including normal and friction forces will be transferred only in the case of closed contact. On the other hand, opening of the contact element may lead to divergence. Open or closed contact is determined based on the gap size. The gap size is automatically calculated from the node locations of the gap element during simulation or from the real constant applied before simulation. In the present analysis, the gap real constant was set to zero ignoring the node locations. Also, some weak springs with  $1e-6N/m$  stiffness have been applied to prevent such divergence.

Tangential movement of the seal in the contact area along the vertical direction is possible. This may happen

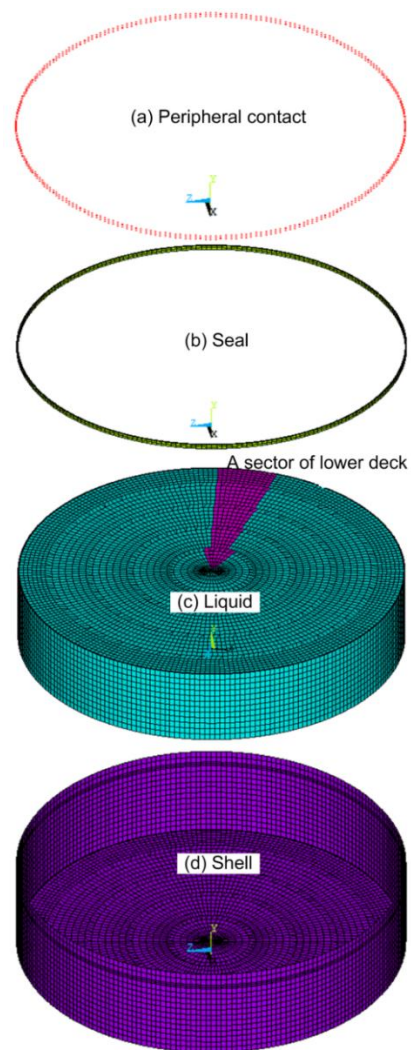


**Figure 11.** Exploded finite element model of the shell, liquid and seal

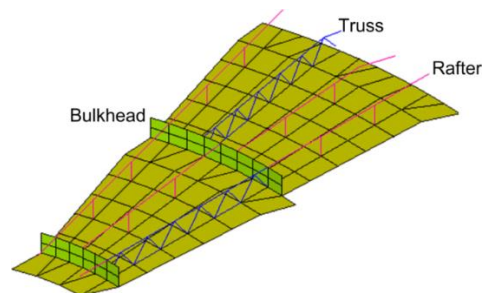


**Figure 12.** Meshing coincidence of the lower deck and stiffeners

in the two ways that was explained with Equation (12). In sticking condition, the seal can move relative to the shell in the vertical direction depending on the tangential stiffness of the seal. However, slippage occurs when the applied tangential force on the node exceeds the friction

force. If during the excitation, the tangential force reduces to less than the friction force, the contact element will return to the sticking state. The amount of the force required for complete slippage of the seal is set to 1000N. In this estimation, the coefficient of friction between nylon and steel (0.6) [31], initial compression of the seals, friction between the weather shield and the shell has been considered. The major challenge in this regard is the seal crumpling due to non-homogeneous slippage of the seal in the circumferential and vertical direction; some nodes of the seal may slip while the adjacent nodes are in the sticking state. This condition leads to the seal crumpling and divergence of the calculation results. To overcome this problem, gradual slippage has been implemented by distributing the tangential contact force to several spring-sliders [26].

Two important conditions must be provided at the roof-liquid interface: the first condition is the roof-liquid FSI, and the other is the sloshing that is transferred to roof. In this regard, there are two kinds of pressure in the liquid adjacent to the roof. The first one is the impulsive pressure, which depends on the speed of sound and appears in the roof-fluid FSI. The other is the convective pressure, which is due to gravity, and appears in the slosh phenomenon.

For FSI establishment, contact elements has been generated between the lower deck and liquid, and then FSI was introduced. For slosh generation, the gravity condition must be satisfied on the liquid upper surface. Presence of gravity acceleration is essential especially for the upper elements of the liquid. Therefore, gravity acceleration was applied to the liquid. Then, sloshing was considered according to Equation (1). For simulation of this phenomenon, displacement-based stiffness elements were generated by adding some vertical springs to the upper surface of the liquid. The other end of each spring must be connected to a node with the same radial position with the upper end and zero vertical displacement. Therefore, the lower ends were connected to the tank bottom nodes. Finally, these springs were omitted in the post-processing. The upper ends of the springs are shown with contact elements in Figure 10d.

So far, finite element model of all the essential components of the tank has been presented. It is intended to discuss the vibration characteristics of the roof in the two cases of seals. For this purpose, modal and time history analysis has been performed to obtain the seismic behavior of the roof, which will be discussed in the next sections.

## 6. MODAL ANALYSIS AND RESPONSE SPECTRUM METHOD

Modal analysis has been conducted in the two sealing cases of the tube and foam seal using the model

introduced so far. The first two dominant natural frequencies resulted from the modal analysis have been summarized in Table 4. In modal analysis, mass and stiffness matrix of the roof is calculated based on its initial stable position. Therefore, the result of the modal analysis is linear with respect to the mass and stiffness matrices. However, time history analysis is non-linear in this respect, which will be discussed later. Hence, the frequency values indicated in Table 4 were revised according to the time history results to achieve the values that are more realistic. For convenience, the first two dominant natural frequencies are indexed as  $fn1$  and  $fn2$ . Comparison of the natural frequencies in the two sealing cases indicates that the amount of the seals participation in the roof vibration is significant. Hence, ignoring them, as in many references, will lead to unrealistic results.

In another row of Table 4, response displacement is mentioned that depends on the magnitude of the earthquake response spectrum at the intended natural frequency. Response spectrum is a function of the frequency spectrum of the earthquake and the damping ratio of the studied system at its natural frequency. Refer to the descriptions provided by Shelke [32, 33] and Versluis [34] for more information about the response displacement and frequency response. Different earthquakes have different frequency spectra. On the other hand, comparison must be accomplished in equal excitation amplitude. In this section, equalization has been done by taking equal spectrum displacements. For this purpose, for each natural frequency, a harmonic excitation was applied with a frequency equal to the considered natural frequency during 20s. The amplitude was considered to be 0.01m for the first natural frequency and 0.001m for the second one. Such amplitudes were equal in both sealing cases. For determination of the roof vibration, modal response was calculated using response spectrum method described above. Modal response represents the maximum amplitude of the system at the intended natural frequency. These values are listed in the last row of Table 4.

Table 4 exhibits that the natural frequency of the roof in the foam sealing case is higher than that in tube sealing case.  $fn1$  frequency for the foam sealing case was 9% higher than that in the tube sealing case. This value was 0.9% for  $fn2$ . This difference is due to the higher shear modulus of the foam seal than the tube seal. Modal responses show that in similar excitation the vibration of the roof in the foam sealing case is lower than that in the tube sealing case. In this regard, modal response of  $fn1$  in the foam sealing case was 18% less than that in the tube sealing case. This value was 20% for  $fn2$ . This difference is due to the more damping ratio of the foam seal in relative to the tube seal.

In response spectrum method, only maximum displacement of the roof was determined at the dominant natural frequencies. In order to know the overall

**TABLE 4.** Dominant natural frequencies of the storage tank in the tube and foam sealing cases and their modal characteristics under horizontal excitation

Sealing case	Tube seal		Foam seal	
Natural frequency index	fn1	fn2	fn1	fn2
Frequency value (in Hz)	0.175	0.725	0.191	0.735
$\gamma$ (Participation factor)	1.116e5	1.128e5	1.242e5	1.276e5
$= \theta_{\max}$ (High spot displacement of the mass normalized mode shape)	0.883e-5	0.849e-5	0.828e-5	0.857e-5
Damping ratio	0.0228	0.0435	0.0484	0.0678
$S_a$ (Response displacement (in m))	0.848	0.108	0.665	0.073
Modal response $= \theta_{\max} \times \gamma \times S_a$	0.836	0.103	0.684	0.080

vibration pattern of roof in modal analysis, mode shape analysis is required.

**7. MODE SHAPES**

Modal analysis exhibited similar mode shapes for the two sealing cases in the first and second dominant natural frequencies. Therefore, only the roof mode shapes in the foam sealing case have been demonstrated. In Figures 13 and 14, the first and second mode shapes of the roof have been shown respectively. In these figures, maximum absolute displacements are indicated by ‘MX’ and ‘MN’. Hereafter, this area will be referred to as ‘high spot’ so as not to be mistaken with the time wave peak. These figures showed that the high spots of the mode shapes are located on the upper deck. The lower deck has lower vibration as it is limited on the both sides, and it is thicker than the upper deck. Therefore, high spot of the upper deck will be used hereafter for vibration comparison. ‘MX’ or ‘MN’ spot whichever has more vibration will be selected.

**8. TIME HISTORY ANALYSIS**

In this analysis, time step increments have been used during the application of some excitation time waves. The system specifications and FSI characteristics are similar to the modal analysis. Newmark time integration with Newton-Raphson numerical approach has been taken into account for solution.

The base of the storage tank was excited horizontally by 1999 Izmit earthquake in Sakaria of Turkey taken from SeismoSignal software accelerograms [35]. Izmit earthquake has been selected as an earthquake near Iran,

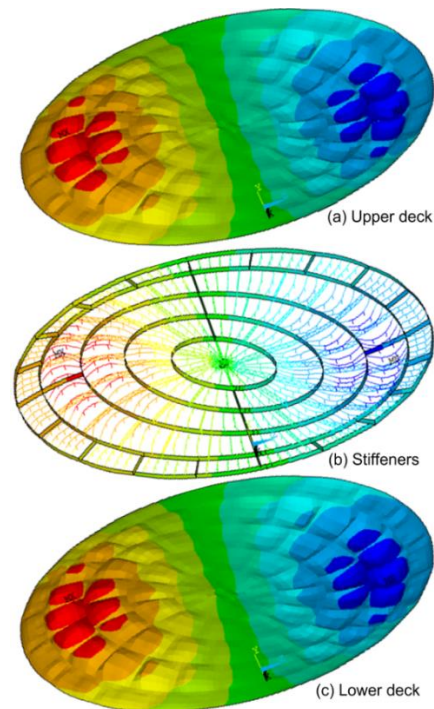


**Figure 13.** First mode shape of the roof

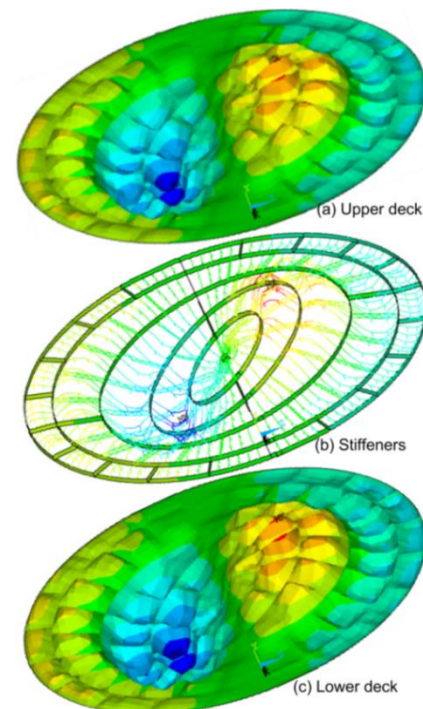


**Figure 14.** Second mode shape of the roof

i.e. the country where the tank is located. This earthquake caused 30 to 45 floating roofed tanks to catch fire due to excessive sloshing [5]. The stated earthquake has a great effect on the first natural frequency of the floating roofs.

Time analysis has been accomplished by ANSYS. 0.03s time steps have been selected for the time history analysis. In Figure 15, time wave of Sakaria earthquake in the horizontal direction is demonstrated. As can be seen, Peak Ground Acceleration (PGA) of the time wave has been scaled to 0.2g.

Maximum vibrations due to the earthquake were occurred in the high spot as mentioned in the modal analysis. Therefore, vibration of this spot was selected for demonstration of the time waves. Figure 16 shows the time domain vibration of the roof at high spot for the tube and foam sealing cases. As the figure shows, the analysis has been performed in 20s for forced vibration simulation and 20s during free vibration. In this figure, more vibration in the tube sealing case than the foam sealing case is evident.

In Figure 17, Fast Fourier Transformation (FFT) of the roof vibration at high spot has been illustrated, which verifies higher vibration of the roof in tube sealing case than the foam sealing case. In this figure, FFT of Sakaria earthquake is also demonstrated. As shown, the vibration in the foam sealing case is lower than that in the tube sealing case despite its excitation value. In this regard, vibration/excitation in the tube sealing case was 0.84, while this value was 0.59 in the foam sealing case during such time duration.

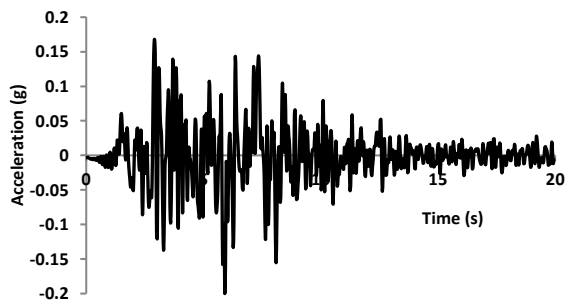


**Figure 15.** Time wave demonstration of the Sakaria earthquake in the horizontal direction

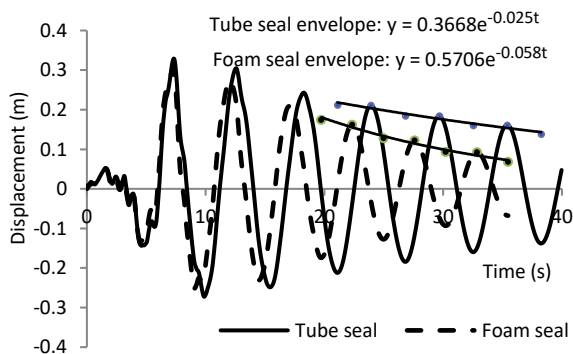


**Figure 16.** Time domain vibration of the roof high spot in the tube and foam sealing cases due to the horizontal component of the Sakaria earthquake

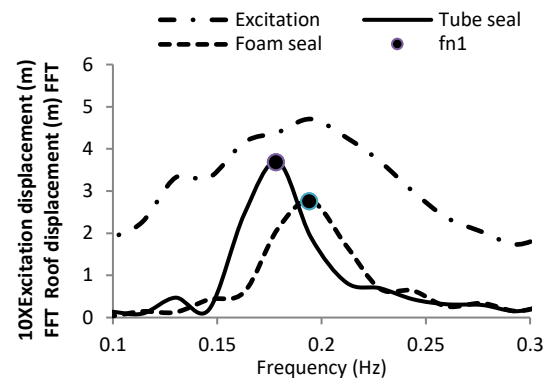


**Figure 17.** FFT of the roof vibration in the tube and foam sealing cases due to the horizontal component of the Sakaria earthquake

So far, vibration displacements of the roof in the tube and foam sealing cases were compared. However, simulation time is also involved in the comparison. Therefore, some manipulation is needed in order to cancel out the involvement of the time in the vibration comparison. In Figures 16 and 17, this was conducted by performing the analysis in equal number of cycles and by continuing the analysis to the free vibration as possible. Lower vibration in the foam sealing case is obvious in this analysis. However, in similar cases where the vibration amplitudes are close to each other, more simulation time is needed. More precise approach is the steady-state method. The governing relationships in the steady-state vibration were developed by Ahmadi and Kadivar [1]. Based on these relationships, the tank was excited with equal harmonic amplitude at a frequency equal to the natural frequency of each sealing case. Simulation time was extended to the steady-state condition to have time-independent evaluation. Vibrations of the roof in the two sealing cases were compared in Figure 18 using this approach. In this vibration simulation, a low equal value of damping has been added to both sealing cases to reach the steady state sooner. It clearly shows that the floating roof has less vulnerability to the seismic vibrations in the foam sealing case.

So far, seismic vibration of the roof showed less vibration vulnerability in the foam sealing case. However, it is required to identify the main factors of the seal, which are effective to the roof vibration. In this regard, parametric study of the seal will be discussed.

### 9. INVESTIGATION OF THE EFFECTS OF THE MECHANICAL PARAMETERS OF THE SEAL ON THE FLOATING ROOF VIBRATION

The main mechanical parameters of the seal are surface slipping, damping, density and elastic and shear modulus.

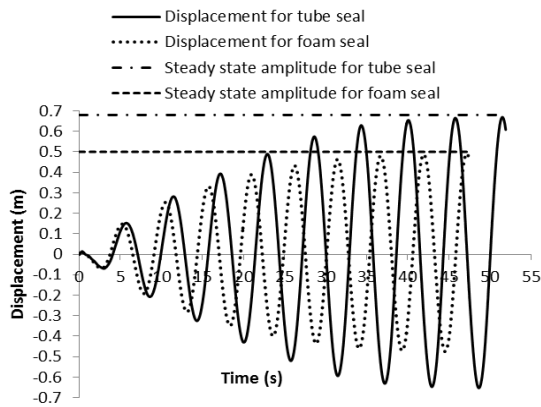


**Figure 18.** Comparison of the steady-state vibration of the roof in the tube and foam sealing cases under harmonic horizontal excitation

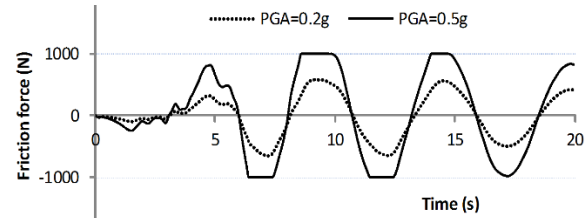
The stiffness of the contact in the sticking state has been taken approximately equal to the seal stiffness. Sakaria PGA has been set to 0.2g so far. In this condition, the contact mechanism was not in the slipping state. Although, there was some vertical movement of the roof periphery with respect to the tank shell. In order to observe the effect of slipping, the PGA was increased to 0.5g. In Figure 19, the difference between these two PGA cases is shown by demonstrating the friction force versus time on the high spot of the foam seal. The slip of the seal at 1000N for the PGA=0.5g is evident in this figure. The phenomenon has been appeared in several peaks when the roof went up and down.

Figure 20 shows friction force distribution of the contact spring-slider at 14.01s during the Sakaria earthquake in the foam sealing case. Several slips can be observed in the red and blue zones as their contact forces reach 1000N.

In the spite the slips shown in Figures 19 and 20, the seal and tank at the contact area had approximately the same radial displacement at most compressive contact area. Figure 21 shows the radial displacement of the seal and the tank shell at such point. In other words, the seal did not have interference with the tank shell, which is desirable for this calculation.

Considering the contact slip present in the 0.5g-scaled excitation, vibration behavior of the roof was analyzed for the two sealing cases in such slipping condition. In Figure 22, the result of such analysis has been demonstrated, and vibration of the roof was compared in the two sealing cases. As can be seen, the vibration amplitudes have been increased by a ratio approximately equal to the PGA ratio, i.e. 0.5g/0.2g. Also, the time periods have not changed. On the other hand, the roof vibration in the foam sealing case is still less than that in the tube sealing case. This investigation shows that the limited slip of the roof does not have significant effect on the roof vibration criteria and the comparison that has been done so far.

Damping ratios were derived from the exponent of the envelope curves in the free vibration part of Figures 16 and 23 that is ' $-\zeta\omega t$ '.



**Figure 19.** Friction force on the high spot of the foam seal for PGA=0.2g and PGA=0.5g

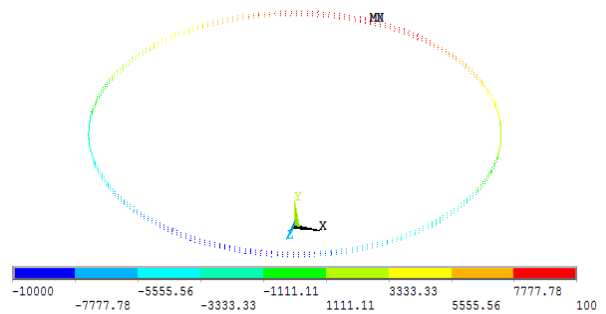


**Figure 20.** Force distribution of the contact spring-slider at 14.01s during Sakaria earthquake in the foam sealing case

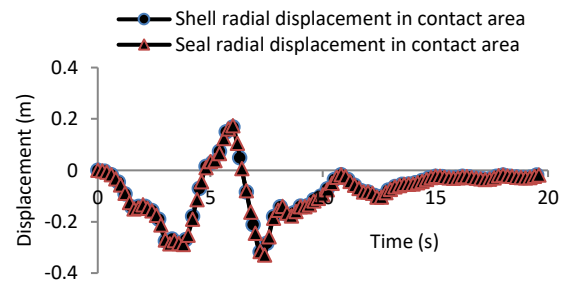


**Figure 21.** Radial displacement of the seal and tank shell at the most compressive contact area

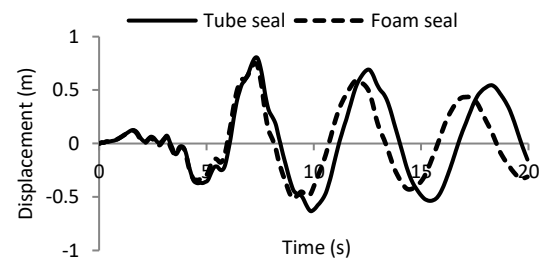


**Figure 22.** Time wave vibration of the roof high spot due to 0.5g-scaled Sakaria earthquake in the tube and foam sealing case

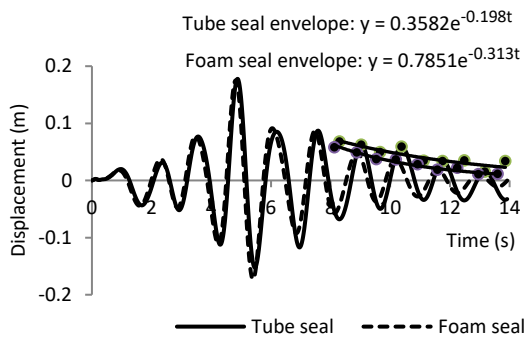


**Figure 23.** Calculation of the logarithmic decrement of the roof at the second natural frequencies in the tube and foam sealing cases

The damping ratios summarized in Table 5 show that they have been increased from the tube sealing case to foam sealing case. This fact exhibits the effect of the foam hysteresis damping on the roof vibration.

Then, the foam density was increased from  $34 \text{ kg/m}^3$ , i.e. the foam seal density, to  $1000 \text{ kg/m}^3$ , i.e. the tube seal density. The vibration of the roof was approximately the same in the two cases as was expected. This is because the seal mass is negligible in comparison to the roof mass.

In the next step, modulus of elasticity of the seal has been increased 10 times without changing shear modulus. This assumption is to observe the effect of the elastic modulus regardless of the shear modulus variation. Although in fact, these two factors are interdependent. The result showed that the roof vibration was approximately equal in the two cases.

After that, assuming anisotropic seal, the shear modulus was increased without elastic modulus change. The vibration of the roof did not change due to the circumferential shear modulus variation. However, the shear modulus change in the vertical (tank-axial) direction resulted in the variation of the natural frequency and participation factor.

The aforementioned studies showed that the seal damping and vertical shear modulus have the most contributions to the roof vibration. Damping ratio of the seal suppresses the roof vibration, and shear modulus increases the natural frequency of the roof. Higher damping ratio of the foam seal with respect to the tube seal leads to more vibration damping of the roof as was observed in Figures 16 and 23. As in many oil industries,

**TABLE 5.** Equivalent damping ratios ( $\zeta$ ) of the first and second natural frequencies for the tube and foam sealing cases

Seal type	$\zeta$ for $fn_1$	$\zeta$ for $fn_2$
Tube	0.0228	0.0435
Foam	0.0484	0.0678

water is selected as the liquid inside the tube. The shear modulus in the tube seal is low as the shear modulus of water is negligible. On the other hand, foam has higher shear modulus than water, which leads to higher shear modulus of the foam seal in comparison to the tube seal.

Based on the above-mentioned results, foam seal is preferred for the roof vibration suppression due to more damping. In addition, it is recommended to add some extra-foam vertically in order to have more damping which leads to a thickened foam seal. Figure 5 shows that the empty space in this region allows the installation of the additional foam. Inclusion of more damping to the seal fixtures or weather shield will also contribute to such vibration suppression. In this regard, damping of the foam seal was assumed to have 50% increment. Note that the total radial initial forces exerted by the foam seal on the tank shell must be kept constant during foam addition. This strategy lets the roof to have smooth vertical movement when the tank liquid level changes. Such foam addition is desirable regarding the cheap price of the foams relative to the other materials used in the storage tank industries and the possibility of the execution. The amount of vibration mitigation has been studied by application of 2017 Sarpol-e Zahab earthquake [36]. Sarpol-e Zahab earthquake is a recent earthquake in the east of Iran, which occurred in the same seismotectonic province of the studied storage tank, i.e. Zagros. The studies conducted by Yazdani and Kowsari [37] predicted high probability density of earthquake occurrence in this province. Earthquake prediction in this province can also be studied using the method presented by Sadeghian and Emamgholi Babadi [38].

Time wave of the horizontal component of this earthquake is demonstrated in Figure 24. This earthquake has been frequency-modulated in order to have equal excitation at the natural frequencies of the ordinary and extra-foam sealing cases. Hence, displacement of the excitation is approximately equal in the two sealing cases. Therefore, in order to have dimensionless comparison, vibration displacement has been analyzed. The result has been demonstrated in Figure 25. This figure compares the time wave displacement of the roof high spot in the ordinary foam and extra-foam sealing cases. Vibration peak has been decreased about 12% due to the extra-foam seal application. However, the natural frequency has been increased. Furthermore, in the thickened foam seal, the third cycle has about 62% decrement with respect to the maximum peak while this value is about 52% in the ordinary foam seal. This fact shows more decay rate of the roof vibration in the thickened foam sealing case.

Note that velocity comparison will also yield the same result, because both the excitation and vibration output must be multiplied by their respective rotational natural frequency, which in turn will lead to the same 'output/input' values.

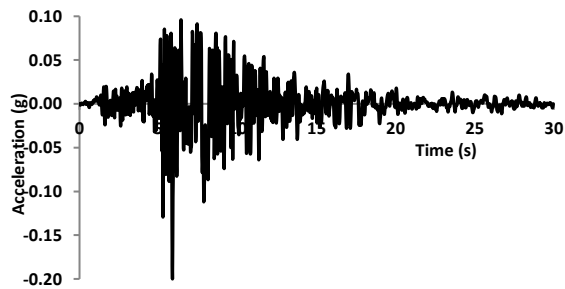


**Figure 24.** Time wave demonstration of the SarPol-e Zahab earthquake in the horizontal direction

The roof horizontal stress was also compared in the two cases of ordinary and extra-foam seal. The most intensive times were selected for the analysis according to Figure 25 time wave. In this figure, vibration peak has been occurred at 10.92s in the ordinary seal and 9.44s for extra-foam seal. These times were selected for stress demonstration of the upper deck. The result is shown in Figures 26 and 27. As it can be seen, the most intensive stress has been occurred at the spot of the seal and tank shell collision in the earthquake direction. This spot is indexed by 'MX' in Figures 26 and 27, and is selected for time simulation of the roof stress in Figure 28. The stress was calculated in the earthquake action direction. This figure also verifies the less severity of the roof in the extra-foam sealing case with respect to the ordinary foam sealing case.

### 10. ANALYSIS OF THE LIQUID BEHAVIOR

To analyze the liquid effect on the roof vibration, the dynamic pressure on the elements adjacent to the liquid surface was investigated. For this purpose, the dynamic pressure at 10.92s under SarPol-e Zahab earthquake for ordinary foam sealing case has been illustrated in Figure 29. Furthermore, vertical displacement of the liquid and some adjacent structures in cutaway views have been demonstrated in Figure 30. Figure 29 shows that the

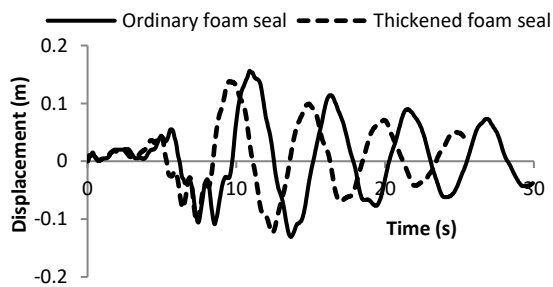


**Figure 25.** Time wave vibration of the roof high spot in the ordinary and thickened (extra) foam sealing cases due to the SarPol-e Zahab earthquake

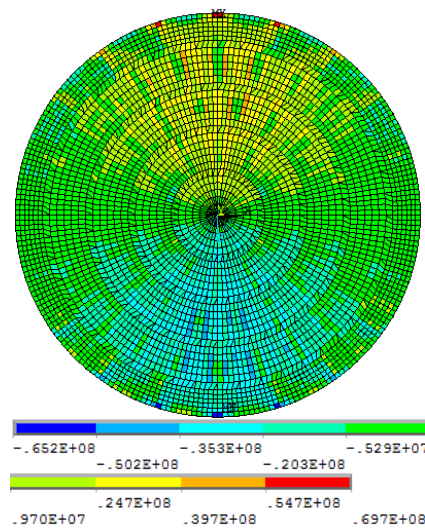


**Figure 26.** Stress pattern of the upper deck at the time of the peak stress (10.92s) due to the SarPol-e Zahab earthquake in the excitation direction in the ordinary foam sealing case

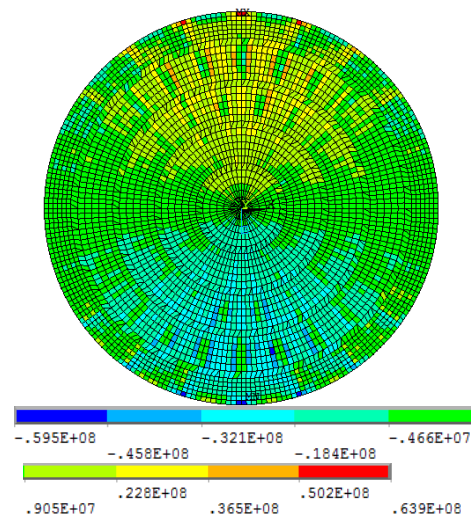


**Figure 27.** Stress pattern of the upper deck at the time of the peak stress (9.44s) due to the SarPol-e Zahab earthquake in the excitation direction in the extra-foam sealing case

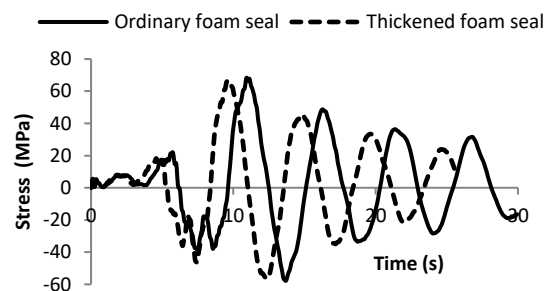


**Figure 28.** Time simulation of the stress of the roof high spot in the ordinary and thickened (extra) foam sealing cases due to the SarPol-e Zahab earthquake

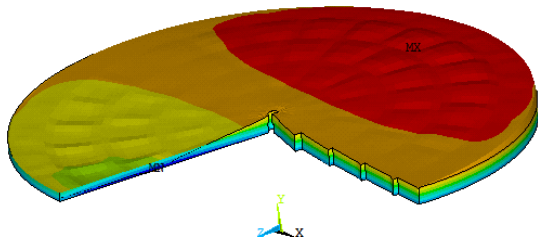


**Figure 29.** Dynamic pressure at 10.92s under SarPol-e Zahab earthquake in the ordinary foam sealing case

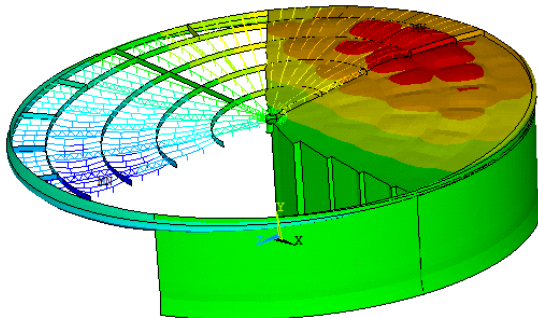


**Figure 30.** Vertical displacement of the liquid and the roof parts under SarPol-e Zahab earthquake at 10.92s in the ordinary foam sealing case

liquid dynamic pressure pattern is consistent with the displacements depicted in Figure 30. In addition, the two latest figures coincide with the first mode shape shown in Figure 13.

**11. VALIDATION OF THE NUMERICAL MODEL**

An attempt was made to validate the results obtained from the modal and time history analysis. However, the present model is significantly different from the previous models of the literature. Such complicated structure of the roof in addition to the contact and slipping behavior have not been proposed in the previous studies. These differences make it difficult to find similar models to verify the results. Hence, the only way is to simplify the present model. In this way, the upper deck and stiffeners have been omitted in the verification, and the natural frequencies were compared with the results obtained from the analytical method recommended in Eurocode 8 part 4 standard [39]. The considered tank was assumed to have fixed conditions at the base as in the present work. However, this analytical approach was recommended for bare tanks. In this work, the equivalent condition for bare tank has been provided by using low-modulus lower deck. In this condition, the first natural frequency of the storage tank was compared with the Eurocode 8 part 4 standard. The result of such comparison has been summarized in Table 6. In this table, the natural frequencies are converged to the values close to the

natural frequency computed by Eurocode 8 along with the reduction of the elastic modulus of the lower deck.

As described before, two methods have been used for vibration severity calculation: response spectrum and time history methods. In the response spectrum approach, the maximum vibration peak is calculated at the considered natural frequency. In the time history analysis, this quantity can also be derived from the time wave vibration data. Time wave vibration curves showed that the first natural frequency is the dominant part of the maximum vibration peak. Hence, comparison of the vibration peak obtained by these two approaches is possible. In Table 7, these two results are summarized for the foam sealing case under the excitation of Sakaria and SarPol-e Zahab earthquakes. As can be seen, the right and left columns have good compatibility.

For time history validation, it is difficult to find a similar seismic wave rather than finding the same model with the one used in the references, as the earthquake records used in the literature do not have accurate addressing of the station. Small frequency deviation from the first natural frequency may lead to a significant vibration difference of the roof. However, the present time history analysis was compared with the model studied by Moslemi and Kianoush [40] under the 1940 El Centro earthquake. The available data from this earthquake was found to be similar with the one used in the reference as possible. Refer to the aforementioned analysis to find the specifications of the model studied by the authors. As can be seen, the storage tank was a concrete shell containing water without floating roof. The present model was changed to the studied model. However, the lower deck has also been added to the

**TABLE 6.** Comparison of the natural frequencies calculated by Eurocode 8 and the present method in the absence of the upper deck and stiffeners

Frequency Index	fn1 (in Hz)	fn2 (in Hz)
Eurocode 8 method	0.0978	0.2072
$E_{lower\ deck} = 2e11\text{Pa}$	0.1036	0.2235
$E_{lower\ deck} = 2e8\text{ Pa}$	0.1016	0.2197
$E_{lower\ deck} = 2e5\text{ Pa}$	0.1016	0.2195

**TABLE 7.** Comparison of the maximum vibration peak obtained by response spectrum and time history methods

Excitation type	Modal response by response spectrum method	Vibration peak by time history analysis
Sakaria earthquake	0.302	0.304
SarPol-e Zahab earthquake	0.150	0.156

system to check the validity of FSI and the dynamic behavior of the selected part of the roof. As Figures 31 and 32 show, high spot vibration of the lower deck conforms approximately with the high spot vibration of the liquid surface calculated by Moslemi and Kianoush.

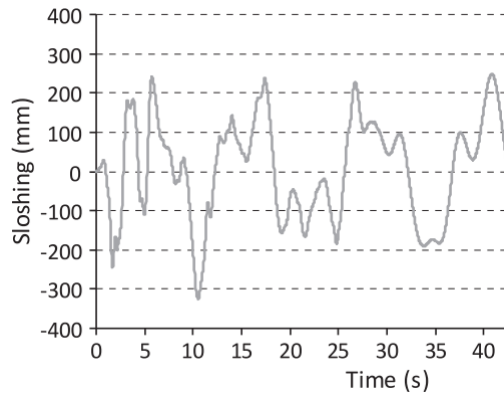


**Figure 31.** Time wave vibration of the liquid surface high spot due to 1940-El Centro earthquake with 0.4g scaling calculated by Moslemi and Kianoush

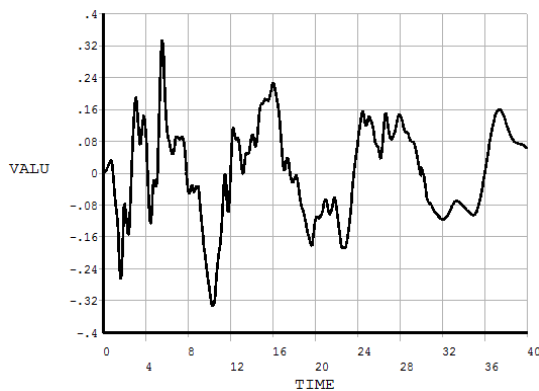


**Figure 32.** Time wave vibration of the lower deck high spot due to 1940-El Centro earthquake with 0.4g scaling calculated in the present study (This figure is the ANSYS output in which 'VALU' is displacement in meter, and 'TIME' is in second.)

## 12. CONCLUSION

To study and compare the seismic behavior of the floating roof in the tube and foam sealing cases, modal and time history analysis have been performed .

In modal analysis, hydroelastic natural frequencies of the floating roof, mode shapes and modal responses were obtained, which led to the following results.

1. The first and second natural frequencies in the foam sealing case were higher than that in tube sealing case.
2. The mode shapes of the dominant natural frequencies were similar in the two sealing cases.

3. In equal harmonic excitation, modal response of the first and second natural frequencies in the foam sealing case was less than that in the tube sealing case.

In time history analysis, the storage tank was excited by the horizontal component of Sakaria earthquake and two harmonics with equal amplitude at the first natural frequency of each sealing case through which the following results were achieved.

1. Vibration/excitation of the first and second natural frequencies in the foam sealing case was lower than that in the tube sealing case.
2. Steady state amplitude due to the harmonic excitation in the foam sealing case was lower than that in the tube sealing case.

It was concluded from the above modal and time history analysis that the floating roof is less vulnerable to seismic vibration in the foam sealing case than in tube sealing case. To identify the contribution of the seal factors to this phenomenon, mechanical parameters of the seal including elastic and shear modulus, density, damping and slipping has been investigated. In this regard, it was concluded that

1. The hysteresis damping in the foam seal is the cause of the vibration mitigation of the roof in this sealing case.
2. More vertical shear modulus of the foam seal than the tube seal is the main factor in increment of the natural frequency.
3. Slip of the seal periphery does not change the aforementioned conclusion.
4. The effect of the other factors of the seal on the roof vibration is negligible.

Regarding the above achievements, the foam damping was assumed to be increased by 50% by addition of some foam in the vertical direction. Time history analysis of the roof vibration has been carried out with the new revised foam seal by excitation of the tank with the horizontal component of the SarPol-e Zahab earthquake. Numerical results shows that the vibration of the roof in the thickened foam sealing case is considerably lower than that in the ordinary foam sealing case. The above extra-foam addition has been recommended as an approach for more vibration mitigation of the roof.

## 13. REFERENCES

1. Ahmadi, H. and Kadivar, M.H., "Seismic analysis of double deck floating roofs of siraf storage tanks with condensate, light and heavy crude oils", *International Journal of Engineering, Transactions A: Basics*, Vol. 34, No. 10, (2021), 2319-2331, doi: 10.5829/ije.2021.34.10a.13
2. Kuan, S.Y., "Design, construction and operation of the floating roof tank", University of Southern Queensland, Mechanical and Mechatronic Engineering, Australia, Bachelor of Engineering, (2009); Available from: <https://eprints.usq.edu.au/8503>
3. Trimulyono, A., Chrismiando, D., Samuel, S. and Aslami, M.H., "Single-phase and two-phase smoothed particle hydrodynamics

- for sloshing in the low filling ratio of the prismatic tank", *International Journal of Engineering, Transactions B: Applications*, Vol. 34, No. 5, (2021), 1345-1351, doi: 10.5829/IJE.2021.34.05B.30
4. Chang, J.I. and Lin, C.-C., "A study of storage tank accidents", *Journal of Loss Prevention in the Process Industries*, Vol. 19, No. 1, (2006), 51-59, doi: 10.1016/j.jlp.2005.05.015
  5. Hatayama, K., "Lessons from the 2003 tokachi-oki, japan, earthquake for prediction of long-period strong ground motions and sloshing damage to oil storage tanks", *Journal of Seismology*, Vol. 12, No. 2, (2008), 255-263, doi: 10.1007/s10950-007-9066-y
  6. Utsumi, M., "Vibration reduction of a floating roof by dynamic vibration absorbers", *Journal of Pressure Vessel Technology*, Vol. 133, No. 4, (2011), doi: 10.1115/1.4002923
  7. Kobayashi, N., Sato, T. and Torisaka, A., "Passive control of liquid sloshing in floating roof tank with multi dynamic absorber", in ASME 2013 Pressure Vessels and Piping Conference. Vol. 8: Seismic Engineering, (2013), doi: 10.1115/pvp2013-97229
  8. Hasheminejad, S.M. and Mohammadi, M.M., "Active sloshing control in a smart flexible cylindrical floating roof tank", *Journal of Fluids and Structures*, Vol. 66, (2016), 350-381, doi: 10.1016/j.jfluidstructs.2016.07.022
  9. Esfandian, H., Goodarziyan Urimi, M. and Shokoohi Rad, A., "Risk assessment of gasoline storage unit of national iranian oil product distribution company using phast software", *International Journal of Engineering, Transactions A: Basics*, Vol. 34, No. 4, (2021), 763-768, doi: 10.5829/IJE.2021.34.04A.02
  10. Salarieh, H., shabani, r. and tariverdilo, s., "Effect of flexural and membrane stiffness on the analysis of floating roofs", *International Journal of Engineering, Transactions A: Basics*, Vol. 23, No. 1, (2010), 57-64; Available from: [https://www.ije.ir/article\\_71832.html](https://www.ije.ir/article_71832.html)
  11. Shabani, R., "Stress patterns in single deck floating roofs subjected to ground motion accelerations", *International Journal of Engineering, Transactions C: Aspects*, Vol. 26, No. 12, (2013), 1495-1504, doi: 10.5829/idosi.ije.2013.26.12c.10
  12. Yoshida, S., Sekine, K. and Mitsuta, T., "Axisymmetric finite element analysis for sloshing response of floating roofs in cylindrical storage tanks", *Journal of Environment and Engineering*, Vol. 5, No. 1, (2010), 27-38, doi: 10.1299/jee.5.27
  13. Yoshida, S., Sekine, K. and Iwata, K., "Sloshing characteristics of single deck floating roofs in aboveground storage tanks: Natural periods and vibration modes", in ASME 2009 Pressure Vessels and Piping Conference. Vol. Volume 7: Operations, Applications and Components, (2009), 191-199, doi: 10.1115/pvp2009-77187
  14. Golzar, F.G., Shabani, R., Tariverdilo, S. and Rezazadeh, G., "Sloshing response of floating roofed liquid storage tanks subjected to earthquakes of different types", *Journal of Pressure Vessel Technology*, Vol. 134, No. 5, (2012), doi: 10.1115/1.4006858
  15. Shabani, R. and Golzar, F.G., "Large deflection analysis of floating roofs subjected to earthquake ground motions", *Nonlinear Analysis: Real World Applications*, Vol. 13, No. 5, (2012), 2034-2048, doi: 10.1016/j.nonrwa.2011.12.026
  16. Goudarzi, M.A., "Seismic behavior of a single deck floating roof due to second sloshing mode", *Journal of Pressure Vessel Technology*, Vol. 135, No. 1, (2012), doi: 10.1115/1.4007291
  17. Ali Goudarzi, M., "Attenuation effects of a single deck floating roof in a liquid storage tank", *Journal of Pressure Vessel Technology*, Vol. 136, No. 1, (2013), doi: 10.1115/1.4025344
  18. Goudarzi, M.A., "Seismic design of a double deck floating roof type used for liquid storage tanks", *Journal of Pressure Vessel Technology*, Vol. 137, No. 4, (2015), DOI: 10.1115/1.4029111
  19. Meera, U.S. and Reshmi, P.R., "Dynamic analysis of single deck floating roof with deck stiffeners", *International Research Journal of Engineering and Technology (IRJET)*, Vol. 04, No. 04, (2017), 3522-3526; Available from: <https://www.irjet.net/archives/V4/i4/IRJET-V4I4844.pdf>
  20. Golzar, F.G., Shabani, R. and Tariverdilo, S., "Stress analyses in single deck and double deck floating roofs subjected to earthquake ground motions", *Scientia Iranica*, Vol. 24, No. 2, (2017), 727-739, doi: 10.24200/sci.2017.4057
  21. Belostotsky, A.M., Akimov, P.A. and Afansyeva, I.N., "Multilevel methodology of numerical seismic analysis of coupled systems "foundation – shell – pontoon (floating roof) – column(s) – fluid"", *Procedia Engineering*, Vol. 153, (2016), 89-94., doi: 10.1016/j.proeng.2016.08.085
  22. Hosseini, M., Soroor, A., Sardar, A. and Jafarieh, F., "A simplified method for seismic analysis of tanks with floating roof by using finite element method: Case study of kharg (southern iran) island tanks", *Procedia Engineering*, Vol. 14, (2011), 2884-2890, doi: 10.1016/j.proeng.2011.07.363
  23. Sakai F., I.R., "Some considerations on seismic design and controls of sloshing in floating-roofed oil tanks", in The 14th World Conference on Earthquake Engineering, Beijing, China., (2008)
  24. Hosseini, M., Goudarzi, M.A. and Soroor, A., "Reduction of seismic sloshing in floating roof liquid storage tanks by using a suspended annular baffle (SAB)", *Journal of Fluids and Structures*, Vol. 71, (2017), 40-55, doi: 10.1016/j.jfluidstructs.2017.02.008
  25. Ruiz, R., "A new type of tuned liquid damper and its effectiveness in enhancing seismic performance: Numerical characterization, experimental validation, parametric analysis and life-cycle based design. (2015); Available from: <https://repositorio.uc.cl/handle/11534/21185>
  26. ANSYS.Inc. *Customer support / ansys*. [cited 04 May 2022]; Available from: <https://www.ansys.com/support>
  27. Sigrist, J.-F., "Fluid-structure interaction: An introduction to finite element coupling, John Wiley & Sons, (2015)
  28. Beer, F., Jr. Johnston, E.R., DeWolf, J. and Mazurek, D., "Mechanics of materials, McGraw-Hill Education, (2011)
  29. Alzoubi, M., Al-Waked, R. and Tanbour, E., "Compression and hysteresis curves of nonlinear polyurethane foams under different densities, strain rates and different environmental conditions", *Journal of Mechanical Engineering*, Vol. Volume 9, No., (2011), 101-109, doi: 10.1115/IMECE2011-62290
  30. Tanks, G. *External floating roof tanks*. [cited 04 May 2022]; Available from: <https://www.gsctanks.com>
  31. Watanabe, M. and Yamaguchi, H., "The friction and wear properties of nylon", *Wear*, Vol. 110, No. 3, (1986), 379-388, doi: 10.1016/0043-1648(86)90111-0
  32. Shelke, S., Vankudre, H. and Patil, V., "Comparative evaluation of mode combination methods in seismic analysis using response spectrum method for tank structure using fea-seismic fea", in Applied Mechanics and Materials, Trans Tech Publ. Vol. 110, (2012), 5240-5248, doi: 10.4028/www.scientific.net/AMM.110-116.5240
  33. Norouzi, A.H., Gerami, M., Vahdani, R. and Sivandi-Pour, A., "Effects of multiple structure-soil-structure interactions considering the earthquake waveform and structures elevation effects", *International Journal of Engineering, Transactions B: Applications*, Vol. 33, No. 5, (2020), 744-752, doi: 10.5829/ije.2020.33.05b.05

34. Versluis, M., "Hydrodynamic pressures on large lock structures", Delft University of Technology, Civil Engineering and Geosciences, Netherlands, Master of Science, (2010)
35. Seismosoft.Co. *Seismosignal support*. cited 04 May 2022]; Available from: <https://seismosoft.com/support/seismosignal-support>
36. *Iran road, housing & urban development research center: Iran strong motion network*. [cited 04 May 2022]; Available from: <https://smd.bhrc.ac.ir/Portal/en/Search/BigQuakes>
37. Yazdani, A.-. and Kowsari, M., "Statistical prediction of the sequence of large earthquakes in iran", *International Journal of Engineering, Transactions B: Applications*, Vol. 24, No. 4, (2011), 325-336., doi: 10.5829/idosi.ije.2011.24.04b.03
38. Sadeghian, T. and E. Babadi, M., "Earthquake prediction modeling using dynamic changes (case study: Alborz region)", *International Journal of Engineering, Transactions B: Applications*, Vol. 34, No. 2, (2021), 355-366, doi: 10.5829/ije.2021.34.02b.07
39. Committee, E., *Eurocode 8- design of structures for earthquake resistance- part 4: Silos, tanks and pipelines*, in *Specific principles and application rules for tanks*. 2006, European Committee for Standardization: Brussels.81; Available from: <https://www.phd.eng.br/wp-content/uploads/2014/12/en.1998.4.2006.pdf>
40. Moslemi, M. and Kianoush, M.R., "Parametric study on dynamic behavior of cylindrical ground-supported tanks", *Engineering Structures*, Vol. 42, (2012), 214-230, doi: 10.1016/j.engstruct.2012.04.026.

---

### Persian Abstract

---

#### چکیده

ارتعاش سقف شناور در دو حالت آب‌بند تیوبی و فومی بوسیله نرم‌افزار انسیس تحلیل شده است. اندرکنش سیال و سازه و پدیده اسلاش لحاظ گردیده است. پاسخ‌های مودال، موج‌های زمانی و طیف‌های فرکانسی ارتعاش سقف در دو حالت آب‌بندی طی تحریک لرزه‌ای افقی کف مخزن ارزیابی شد. سپس، تأثیر عوامل مکانیکی اصلی آب‌بند بر لرزش سقف بررسی گردید. ارتعاش سقف در حالت آب‌بند فومی به طور قابل توجه از حالت آب‌بند تیوبی کمتر بود که ناشی از میرایی بیشتر آب‌بند فومی نسبت به آب‌بند فومی می‌باشد. همچنین، فرکانس طبیعی حالت آب‌بند فومی از فرکانس طبیعی حالت آب‌بند تیوبی بیشتر بود که به علت مدول برشی بیشتر آب‌بند فومی در راستای عمودی (محور مخزن) می‌باشد. با توجه به این نتیجه، آب‌بند فومی در راستای عمودی خلاصی موجود افزایش داده شد و کف مخزن دوباره تحت تحریک لرزه‌ای قرار گرفت. ملاحظه شد این ارتقاء به لرزه‌گیری بیشتر سقف کمک می‌نماید.

---